Long distance proton transfer with a break in the bacteriorhodopsin active site

Prasad Phatak[1], Jan S. Frähmcke[1], Marius Wanko[2], Michael Hoffmann[2], Paul Strodel[3]
Jeremy Smith[5,6,7], Sándor Suhai[4], Ana-Nicoleta Bondar[4,5,8,#,*], Marcus Elstner[1,4,†]

[1] Institute of Physical and Theoretical Chemistry,
TU Braunschweig, D-38106 Braunschweig, Germany

[2] BCCMS, Universität Bremen, D-28334 Bremen, Germany

[3] Accelrys Ltd., Cambridge CB4 0WN, United Kingdom

[4] Molecular Biophysics Department, German Cancer Research Institute,
Im Neuheimer Feld 280, D-69120, Heidelberg, Germany

[5] Computational Molecular Biophysics, IWR, University of Heidelberg,
Im Neuenheimer Feld 368, D-69120, Heidelberg, Germany

[6] Center for Molecular Biophysics, Oak Ridge National Laboratory,
PO BOX 2008 MS6164, Oak Ridge, Tennessee 37831, USA

[7] Department of Biochemistry and Molecular Biology,
University of Tennessee, M407 Walters Life Sciences,
1414 Cumberland Ave, Knoxville Tennessee 37996, USA

[8] Deptartment of Physiology and Biophysics and the Center for Biomembrane Systems,
University of California at Irvine, Irvine, CA 92697, USA

[#] Present address: Deptartment of Physiology and Biophysics and
Center for Biomembrane Systems, University of California at Irvine, Irvine, CA 92697, USA

[*] Corresponding author. Email address: nicoleta.bondar@uci.edu

[†] Corresponding author. Email address: m.elstner@tu-bs.de

(Dated: March 18, 2009)

I. CALCULATION OF ν_{COOH} MODE WITH GAS-PHASE MODELS

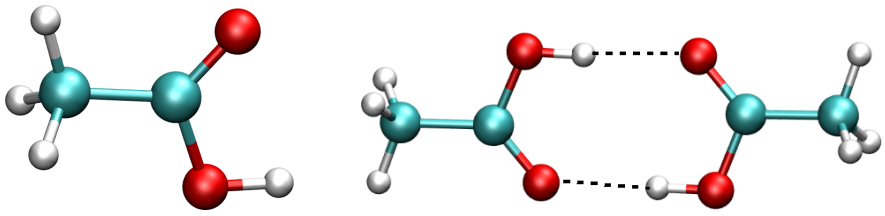

(a) (b)

FIG. S-1: Gas Phase models for carboxylate using acetic acid. (a) An isolated molecule in the protonated state; (b) Two acetic acid molecules forming cyclic dimer with strong hydrogen bonds.

TABLE S-1: Symmetric C=O stretch frequencies (cm^{-1}) of gas-phase models

Model	Calculated value (cm^{-1})	Experimental value (cm^{-1})[a]	shift (cm^{-1})
Acetic acid(aa)	1778	1780	2
Cyclic aa dimer	1708	1725	17

[a] For review see[1]

We performed normal mode analysis for isolated acetic acid molecule (Figure S-1a) and strongly hydrogen-bonded cyclic acetic acid dimer sytem (Figure S-1b) in gas-phase to benchmark SCC-DFTB for ν_{COOH} mode. The results are summarized in Table S-1. For isolated acetic acid molecule, the ν_{COOH} band (1778 cm^{-1}) calculated with SCC-DFTB shows excellent agreement with the experimental value of 1780 cm^{-1} and suggests an upper limit for an isolated Asp residue in O or [O] state. For strongly hydrogen bonded cyclic dimer however, the ν_{COOH} band (1708 cm^{-1}) is red-shifted by 17 cm^{-1} relative the experimental value of 1725 cm^{-1}. In presence of protein environment with surrounding hydrogen bonds, the strong red-shift of 17 cm^{-1} thus suggest a lower bound to the shift of ν_{COOH} mode for Asp residue in O or [O] state.

II. DETAILS OF THE MOLECULAR DYNAMICS (MD) SIMULATIONS

The MD simulations (classical and QM/MM) were initiated starting from the crystal structure of acid-blue bacteriorhodopsin[2]. Equilibrium simulations with stochastic boundary condition and explicit solvent were carried out using CHARMM package (version: c32a2).[3]

TABLE S-2: Isotropic fluctuations of the selected atoms of the QM region from the active-site. QM region consits of retinal, Asp85, Asp212 and 3 waters

Protein group	Atom	Fluctuation (Å)
Ret216	C^{γ}	0.31053
Ret216	C^{δ}	0.38365
Ret216	C^{ϵ}	0.62881
Ret216	N^{ζ}	0.51273
Asp85	C^{β}	0.37463
Asp85	C^{γ}	0.40401
Asp85	$O^{\delta 1}$	0.47970
Asp85	$O^{\delta 2}$	0.48724
Asp212	C^{β}	0.40202
Asp212	C^{γ}	0.43089
Asp212	$O^{\delta 1}$	0.48866
Asp212	$O^{\delta 2}$	0.50671
w401*	O	0.53625
w603	O	0.72482
w406*	O	1.93082

In all cases, the system was partitioned into a 22 Å spherical inner region around N_{ϵ} atom of Arg82 while the remaining region was treated as outer region following the GSBP approach.[4–6] Newtonian equations-of-motion were solved for the molecular dynamics region (within 18 Å), and Langevin equations-of-motion were solved for the buffer region (18-22 Å) with a temperature bath of 300 K.[7]. Protein atoms at the boundary between inner and outer regions are constrained following previously described protocol.[4] For classical MD simulations (3 independent 5-ns trajectories), all bonds involving hydrogen for were constrained using SHAKE[8] to allow a 1-fs timestep. For QM/MM MD simulations (3 independent 1-ns trajectories), QM level is SCC-DFTB[9] and the third-order extension of SCC-DFTB[10] was used which was found to be important for improving the proton affinity.[10] The QM region consisted of complete retinal, Asp85, Asp212, Lys216 side chain and 3 water molecules (w401*, w603, and w406*). All bonds involving hydrogen atoms outside the QM region were

constrained to allow 1-fs timestep.

III. GEOMETRICAL DATA FROM THE QM/MM-MD SIMULATIONS OF MODEL-A^{3w}

In order to investigate the stability of three active-site waters in model-A^{3w}, we carried out QM/MM molecular dynamics simulations for 1ns timescale. The fluctuations around equilibrium values of selected atoms from the qm region are tabulated in Table S-2. The fluctuations of most the atoms from the protein groups of the QM region are within ∼0.3 Å-0.7 Å range. Although all three waters are stable in the active-site, large fluctuations are observed for these waters: w401* (0.5 Å), w603 (0.7 Å) and w406* (1.9 Å) and suggest increased mobility of the waters probably due to presence of an extra proton relative to the bR resting state.[11]

IV. MODELS WITH ONE ACTIVE-SITE WATER MOLECULE

A. PT in model-A^{1w} in presence of Tyr57:Asp212 hydrogen bond

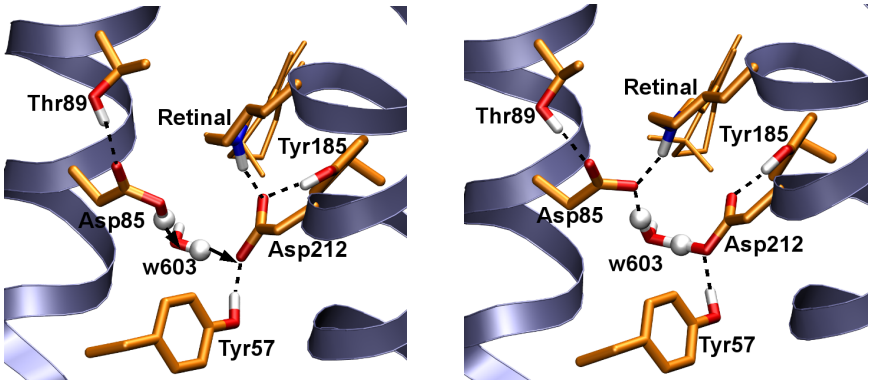

(a)model-A^{1w}-O (b)model-A^{1w}-[O]

FIG. S-2: End states of model-A^{1w} in presence of Tyr57:Asp212 hydrogen bond.

In presence of the Tyr57:Asp212 hydrogen bond the Asp85:Asp212 distance reduces from 4.2 Å in the crystal structure to 3.7 Å in model-A^{1w}-O conformer (Figure S-2a). The vibrational calculations indicate for the O conformer, the ν_{COOH} band (1701 cm^{-1}) is nearly same as the ν_{COOH} band in model-A^{1w} without Tyr57:Asp212 hydrogen bond (1690 cm^{-1}),

while in [O] conformer as a result of shared proton between w603 and Asp212, the ν_{COOH} band is strongly red-shifted to 1551 cm^{-1}. In model-A^{1w}-[O], the proton is shared between w603 and Asp212 (Figure S-2b). The PT from Asp85 to Asp212 via w603 is endothermic and the rate-limiting energy barrier of 4.6 kcal/mol (at λ=0.67 in Figure S-3) is dominated by energy contribution from $E^{nb}_{QM:MM}$ (5.1 kcal/mol) due to the presence of the Tyr57:Asp212 hydrogen bond.

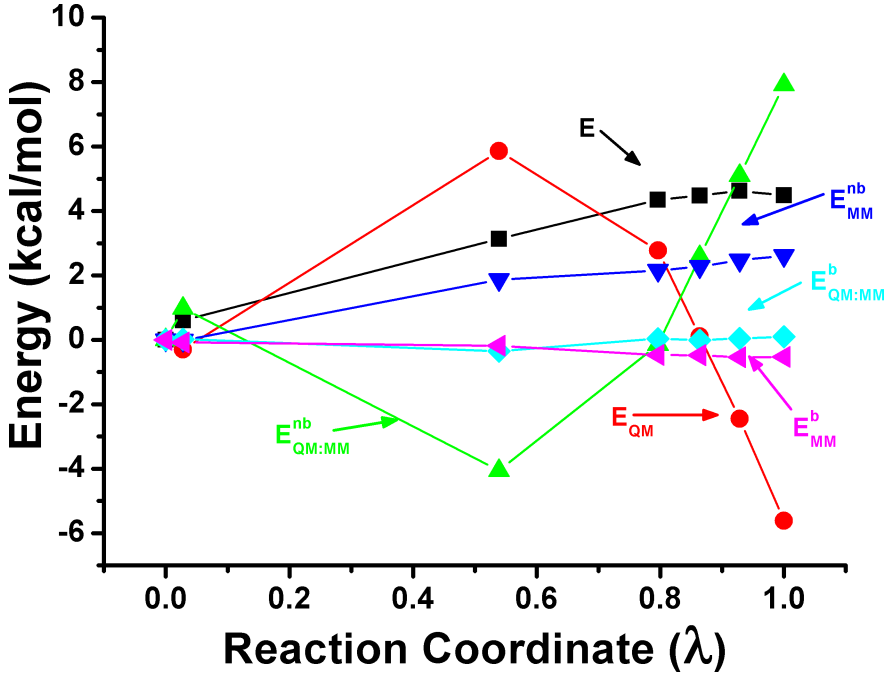

FIG. S-3: Energy decomposition of minimum energy profile for PT in model-A^{1w} in presence of Tyr57:Asp212 hydrogen bond.

B. PT in model-B^{1w}

In the O conformer, the Schiff base forms a salt-bridge with one of the carbonyl oxygen of the acceptor Asp212. The other carbonyl oxygen of Asp212 forms a hydrogen bonded network and involves water w402 and donor Asp85 residue. The reaction begins with change in orientation of the Schiff base which weakens the salt-bridge between the Schiff base and Asp212 residue. Concomitantly, the hydrogen bond between the donor group and w402 strengthens as Asp85 moves closer to the w402. At the transition state (at λ=0.67) (Figure S-4), the w402 is equally shared between the Asp85 (2.4 Å) and acceptor Asp212 (2.4 Å)

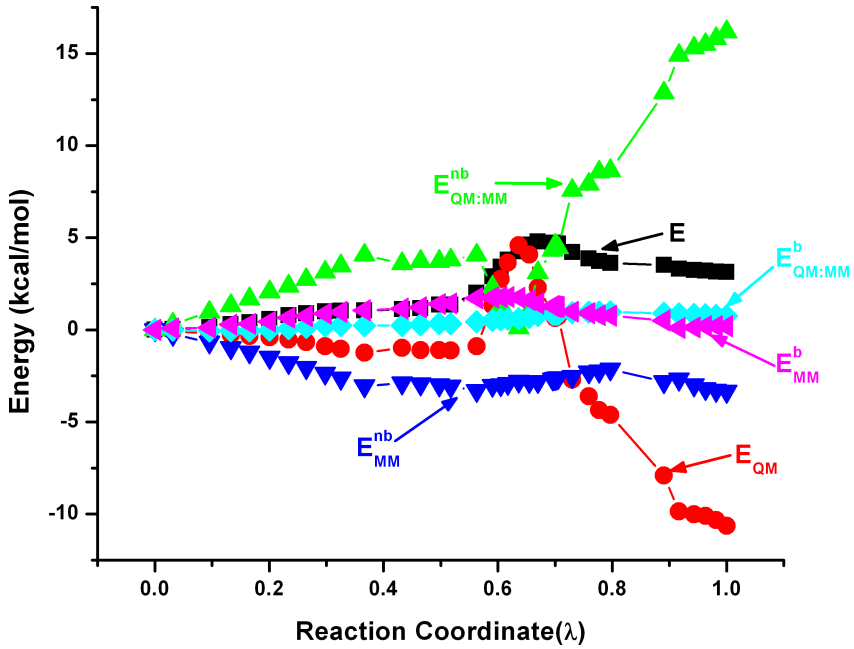

FIG. S-4: Energy decomposition of minimum energy profile for PT in model-B^{1w}

groups following which, the proton is completely transferred from Asp85 to w402 and from w402 to Asp212. The reaction proceeds towards completion with formation of salt-bridge between the Schiff base and the Asp85 residue.

V. MODELS WITH TWO ACTIVE-SITE WATER MOLECULES

A. PT in model-A^{2w}

In model-A^{2w}, the PT takes place from the donor Asp85 residue via water w603 to the acceptor Asp212 residue. In pathway begins as Asp85 while maintaining its hydrogen bond with Thr89 (2.8 Å) orients such that the distance between proton carrying oxygen of Asp85 ($O^{\delta 1}$) and the Schiff base nitrogen reduces from 4.6 Å to 2.9 Å at the transition state (at λ=0.72) (see Figure S-5). The rate-limiting barrier (3.92 kcal/mol) is dominated by opposite sign contributions from E_{QM}(-2.2 kcal/mol) and $E^{nb}_{QM:MM}$(5.1 kcal/mol) and correspond to a shared proton between Asp85/w603 and another proton shared between w603/Asp212. After the PT, a salt bridge is formed between Asp85 and the Schiff base and correspond to almost equal opposite sign contributions from favorable E_{QM} (-18.4 kcal/mol) and unfavorable $E^{nb}_{QM:MM}$ (18.3 kcal/mol).

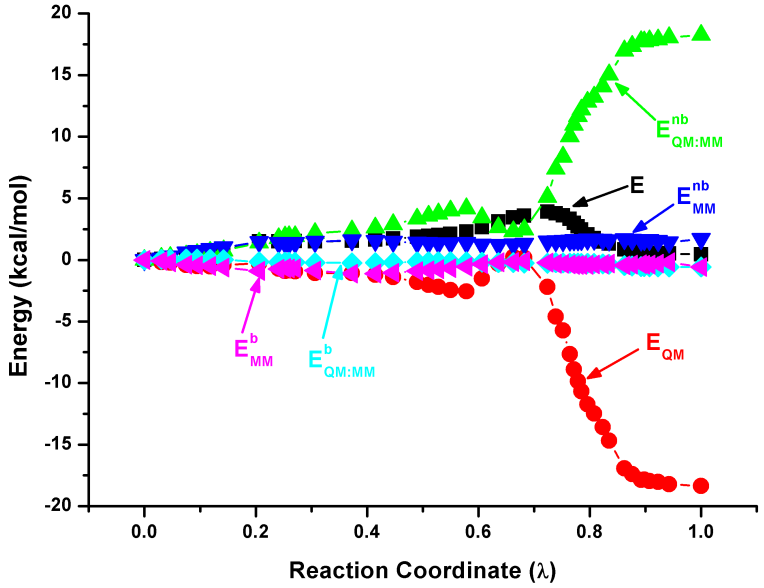

FIG. S-5: Energy decomposition of minimum energy profile for PT in model-A^{2w}

B. PT in model-B^{2w}

The energy profile for the proton transfer pathway in the model-B^{2w} model is shown in Figure S-6. In the beginning of the pathway in model-B^{2w} the hydrogen bond between the Schiff base and w402 breaks as the Schiff base orients away from w402 and towards Asp85. This movement continues till λ=0.64 and involves simultaneous movement of Asp212 such that the distance between the Schiff base and the Asp212-O$^{\delta 2}$ atom increases from 3.4 Å to 4.6 Å. Such increase in the distance between the cationic Schiff base and the anionic Asp212 residue increases the E_{QM} up to 10.5 kcal/mol and decreases the $E^{nb}_{QM:MM}$ by 8.4 kcal/mol. The water w402 then orients to form a hydrogen bond with Asp85 residue. Concomitantly, the proton donor Asp85 moves closer the water W401* such that at the transition state at λ=0.68, the Asp85 shares its proton with water W401* and W401* shares one of its proton with Asp212. Following this, the PT is completed in sequential manner.

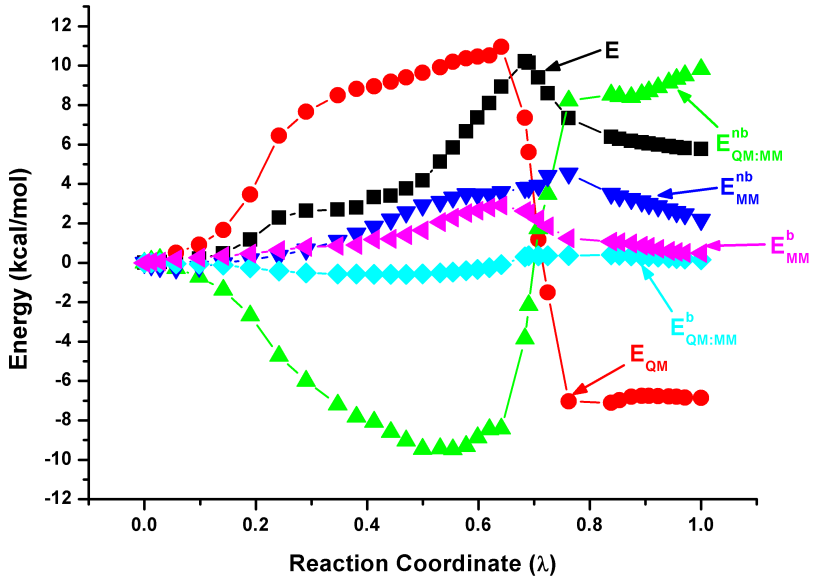

FIG. S-6: Energy decomposition of minimum energy profile for PT in model-B^{2w}

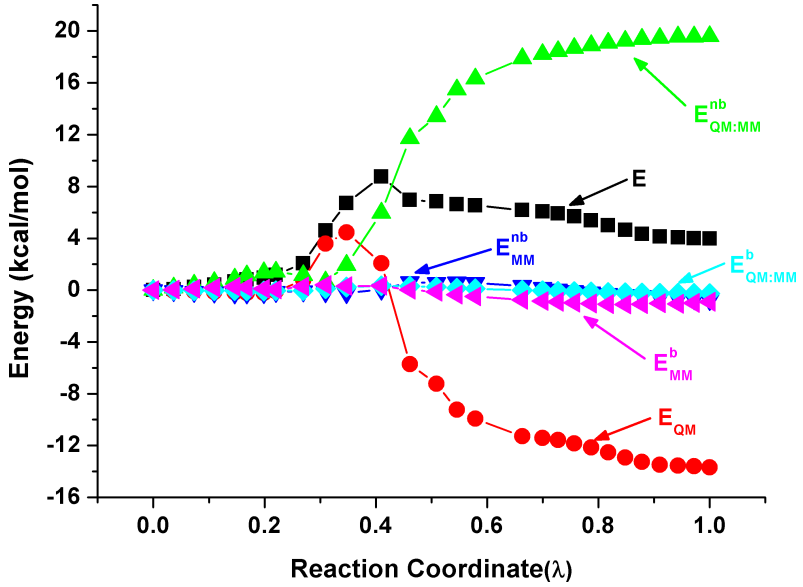

FIG. S-7: Energy decomposition of minimum energy profile for PT in model-B^{3w}

VI. MODELS WITH THREE ACTIVE-SITE WATER MOLECULES

A. PT in model-B^{3w}

In the O state of model-B^{3w}, the distances between the active-site residues Asp85/w401* (2.6 Å), w401*/w406* (2.7 Å) and w406*/Asp212 (2.7 Å) are well optimized for the PT. Thus, the PT reaction proceeds without significant structural change upto λ=0.2 (see Figure S-7) after which, the distance between Asp85/w401*, w401*/w406* and w406*/Asp212 decreases such that at the transition state (at λ=0.41), the proton is shared between Asp85/w401* (2.5 Å), w401*/w406* (2.4 Å) and w406*/Asp212 (2.4 Å) following which the proton is transferred to the Asp212 completing the pathway. In the [O] state, the weak hydrogen bond between Tyr57 and Asp212 (2.7 Å) and Tyr185 and Asp212 (2.7 Å) from 2.6 Å in the reactant is reflected by increase in the $E^{nb}_{QM:MM}$ to 19.6 kcal/mol relative to the reactant. Following the PT in the [O] state, the hydrogen bond between water w402 and Asp212 is broken and a new hydrogen bond between w402 and w406* is formed.

B. PT in model-C^{3w}

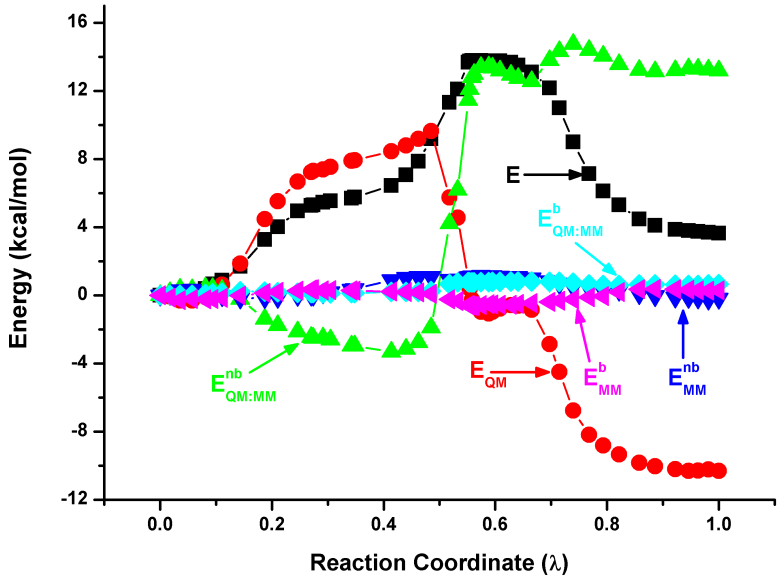

FIG. S-8: Energy decomposition of minimum energy profile for PT in model-C^{3w}

The proton pathway via w402 in model-C^{3w} starts with re-orientation of waters molecules w401 and w406 from Asp212 to Asp85 breaking the hydrogen bond with Asp212. Simultaneously, Asp85 and Asp212 move closer to w402 while w402 maintains its hydrogen bond with Schiff base. Subsequently, at the rate-limiting step (λ=0.56 in Figure S-8), a proton is shared between Asp85 and w402 (2.5 Å) and between w402 and Asp212 (2.5 Å). The PT then finishes with complete transfer of proton from Asp85 to w402 and from w402 to Asp212. The initial contribution to the total energy is dominated by E_{QM} and is due to the orientation of waters breaking the hydrogen bonds between the waters and Asp212. Once the orientation is complete, $E^{nb}_{QM:MM}$ dominates the contribution to the total energy and contributes mainly (13 kcal/mol) to the rate-limiting energy barrier (13.8 kcal/mol located at λ=0.56). The increase in $E^{nb}_{QM:MM}$ is because of the unfavorable electrostatic interactions (11.8 kcal/mol) between the shared water w402 with Asp85 and Asp212 and the surrounding MM groups.

C. PT in model-D^{3w}

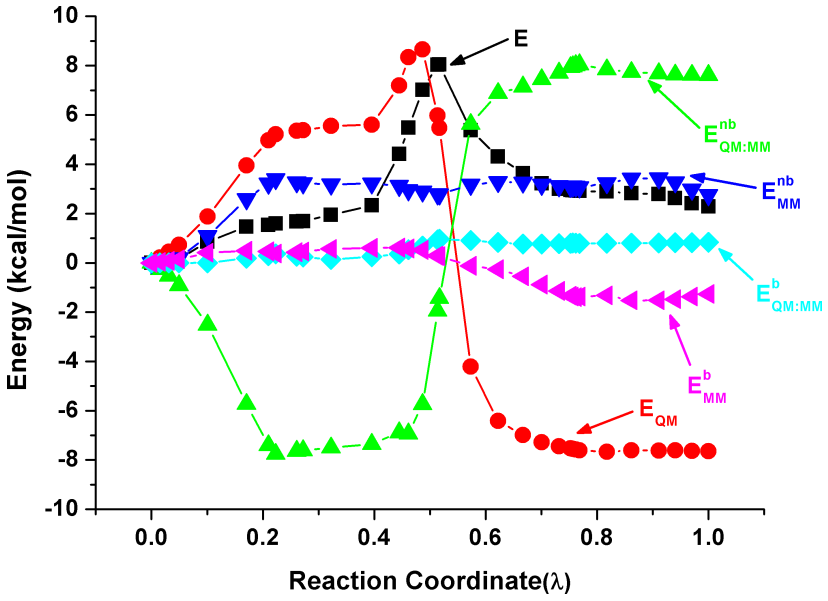

FIG. S-9: Energy decomposition of minimum energy profile for PT in model-D^{3w}

In the O confermer of model-D^{3w}, Thr89 is hydrogen bonded to the backbone carbonyl oxygen of Asp85 and the water w402 to Asp212 and water 406. The pathway begins with orientation of w402 breaking the hydrogen bond with Asp212 and correspond to the increase

in E_{QM} (Figure S-9). Simultaneously, Thr89 orients away from backbone carbonyl Asp85 and forms a hydrogen bond to Asp85 carboxyl oxygen as reflected by sharp decrease in $E^{nb}_{QM:MM}$ (at λ=0.26 in Figure S-9). Following these movements, the proton is transferred in a concerted path from Asp85 to w401, from w401 to w406 and finally from w406 to Asp212. The rate-limiting barrier of 8.0 kcal/mol (at λ=0.52) is dominated by E_{QM} (5.5 kcal/mol) and correspond to the shared proton between Asp85/w401, w401/w406 and w406,Asp212. After the PT, w402 forms hydrogen bond with Asp85 and w406 and correspond to the decrease in E_{QM} while weakening of Tyr57/Asp212 and Tyr185/Asp212 hydrogen bonds from reactant (2.6 Å and 2.6 Å respect.) to [O] (2.7 Å, 2.7 Å respect.) correspond to increase in $E^{nb}_{QM:MM}$ at 7.6 kcal/mol. After the proton is transferred to Asp212, an extracellular water w407 moves to form a hydrogen bond with Thr205 backbone carbonyl oxygen, thus correspond to lowered E^{b}_{MM} energy of -1.3 kcal/mol relative to the reactant.

---

[1] Dioumaev, A.K., *Biochemistry (Moscow)* **2001**, *66*, 1269–1276.

[2] Okumura, H.; Murakami, M. and Kouyama, T., *J. Mol. Biol.* **2005**, *351*, 481–495.

[3] Brooks, B.R.; Bruccoleri, R.E.; Olafson, B.D.; States, D.J.; Swaminathan, S. and Karplus, M., *J. Comp. Chem.* **1983**, *4*, 187–217.

[4] Im, W.; Berneche, S. and Roux, B., *J. Chem. Phys.* **2001**, *114*, 2924–2937.

[5] Riccardi, D.; Schaefer, P.; Yang, Y.; Yu, H.; Ghosh, N.; Prat-Resina, X.; Koenig, P.; Li, G.; Xu, D.; Guo, H.; Elstner, M. and Cui, Q., *J. Phys. Chem. B* **2006**, *110*, 6458–6469.

[6] Schaefer, P.; Riccardi, D. and Cui, Q., *J. Chem. Phys.* **2005**, *123*, 014905–014914.

[7] Brooks III, C. L. and Karplus, M., *J. Mol. Biol.* **1989**, *208*, 159–181.

[8] Rychaert, J.P.; Ciccotti, G. and Berendsen, H.J., *J. Comput. Phys.* **1977**, *23*, 327–341.

[9] Elstner, M.; Porezag, D.; Jungnickel, G.; Elsner, J.; Haugk, M.; Frauenheim, Th.; Suhái. S. and Seifert, G., *Phys. Rev. B* **1998**, *58*, 7260–7268.

[10] Yang, Y.; Yu, H.; York, D.; Cui, Q. and Elstner, M., *J. Phys. Chem. A* **2007**, *111*, 10861–10873.

[11] Hoffmann, M.; Wanko, M.; Strodel, P.; Koenig, P.; Frauenheim, T.; Schulten, K.; Thiel, W.; Tajkhorshid, E. and Elstner, M., *J. Am. Chem. Soc.* **2006**, *128*, 10808–10818.